Rev. Roum. Sci. Techn.– Électrotechn. et Énerg.
Vol. **71**, *2*, pp. 206–210, Bucarest, 2026

SPECIFICS OF SPECTRAL-CURRENT DIAGNOSTICS OF DEFECTS IN INDUCTION MOTOR BEARINGS

VALERII HRANIAK[1], VASYL PONOMARENKO[2]

Keywords: Diagnosis; Higher harmonics; Bearing; Wear; Eccentricity.

The paper theoretically substantiates the influence of defects in motor bearings on the form of their stator current and demonstrates the potential use of amplitude-defined spectral components of stator current as diagnostic indicators for bearing defects. It is shown that during bearing wear, rotor slot harmonics due to eccentricity directly interact with changes in magnetic conductivity across non-uniform air gaps, resulting in significant increases in harmonic amplitudes at rotor speed frequencies. Experimental investigations were conducted to validate these theoretical findings, confirming them comprehensively.

1. INTRODUCTION

During operation, the magnetic field in the stator of an ideal induction motor (IM) exhibits a perfectly symmetrical form. However, in real induction motors, physical parameters deviate from ideal (design) values, inevitably causing deformation of the magnetic field [1]. This deformation alters the magnetic circuit parameters of the IM, leading to dynamic changes in stator circuit parameters, such as resistance and inductance. Consequently, this variation is the cause of the appearance of higher harmonic currents. It is important to note that different types and degrees of deviation of real IM parameters from design specifications will exhibit unique characteristics in their spectral current composition [2]. Since the spectral composition of the stator current is convenient for real-time monitoring, considering the potential functional dependence between its spectral composition and the level of deviation from design parameters (*i.e.*, the degree of defect development), highlights the high potential of current-based diagnostic methods.

2. SETTING THE TASK

The aim of the work is to provide methodological support for improving the operational reliability of induction motors through the development of a theory for building their diagnostic systems, characterized by high sensitivity to the presence of bearing defects while maintaining relative simplicity of structural implementation and low cost.

According to the specified purpose, work tasks are solved:

1. Theoretical justification of the peculiarities of the influence of induction motor bearing defects on the waveform of its stator current;
2. Demonstration of the feasibility of using the amplitudes of specific spectral components of the stator current as diagnostic indicators of bearing defects;
3. Theoretical substantiation of the choice of frequencies of the spectral components of the stator current of an induction motor, for which amplitude growth occurs with the development of bearing defects;
4. Experimental validation of the adequacy of the theoretical conclusions.

3. FORMULATION OF THE PROBLEM

When studying the reliability of a system, it is normally advisable to divide it into structural components with further assessment of the reliability of each of them. At the second stage, such an approach allows determining the system's resulting reliability based on previously established reliability of its structural elements [3]. However, in a typical electromechanical system represented by an electric machine, the probability of individual elements' failure can differ in such a significant way that the overall reliability of the unit will, in fact, be only determined by the reliability parameters of the "weak links" [4, 5]. Considering the said specificity, it is not difficult to conclude on the advisability of focusing only on those types of defects with a higher probability than a certain minimum level while solving the problem of automated control and diagnostics of induction electric motors.

In accordance with the results of statistical analysis of malfunctions that occur during operation of medium-power induction electric motors conducted using the resources of VENTUS.UA company, it can be stated that the bearings' breakdown served as the cause of asynchronous engine's emergency failure in 12% of cases [6]. This gives grounds to consider bearing assemblies as potentially weak links with an increased probability of failure during operation.

It is also worth emphasizing that most of the up-to-date automated control systems intended for induction electric motors already incorporate the functions of on-stator measurement of currents and voltages [7]. Where such a measurement system is not incorporated in the IM control system, its technical implementation will not require intervention into the electric machine's design. Hence, one can conclude that the use of stator current parameters for diagnostics of bearing defects has significant advantages compared to other types of diagnostic systems.

It should also be noted that, as of today, the wide application of this approach is limited by the lack of effective mathematical models that would relate the stator current's spectral composition to bearing assembly defects' presence and degree of development. Therefore, the solution to this scientific and applied problem has great theoretical and practical significance.

4. DEVELOPMENT OF THE MATHEMATICAL DEPENDENCE BETWEEN THE IM STATOR CURRENT'S SPECTRAL COMPOSITION AND BEARING DEFECT PRESENCE

Mechanical defects lead to distortion of the stator current due to load unevenness and magnetic field pulsations. In its turn, the occurrence of magnetic field pulsations is usually associated with a dynamic change in parameters of the IM's magnetic circuit [8, 9].

Bearings are critical elements of the support structure that back up the rotor and ensure its rotation. In low- and

[1]Vinnytsia Mykhailo Kotsiubynskyi State Pedagogical University, Vinnytsia, Ukraine. E-mail: hraniak.valerii@vspu.edu.ua
[2]Taras Shevchenko National University of Kyiv, Kyiv, Ukraine. E-mail: vasylponomarenko@knu.ua

DOI: 10.59277/RRST-EE.2026.2.6

medium-power induction motors, ball bearings consisting of the following components are normally used (Fig. 1): the outer and the inner cage, rolling elements, and the separator. One of the key criteria for assessment of the bearing unit's condition is the bearing's radial clearance. Wear of the rolling elements and the rings' (clamp's) surfaces leads to the radial gap's increase and, as a result, to the rotor's displacement and the air gap's deformation [10].

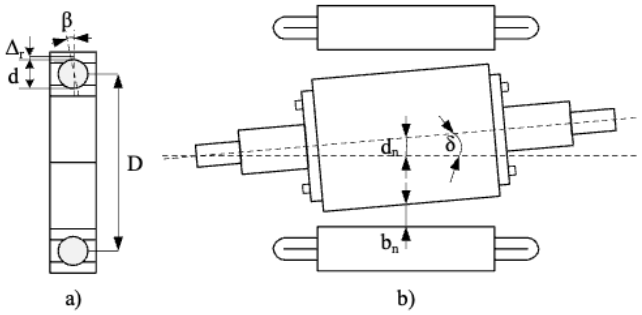

Fig. 1 – Design of the rotor with an uneven air gap: a) rolling bearing; b) rotor's displacement in relation to the stator axis.

Radial clearance Δ_r (Fig. 1) in the bearing is the distance by which the outer bearing cage moves toward the inner cage. At the same time, nominal radial clearance is required to prevent an unwanted tension between the cages and the rolling elements. The increase in the size of the bearings' radial clearance testifies to the raceways' wear as a consequence of the bearing's general wear, and also Fig. 1 shows: d – the rolling element's diameter; β – the contact angle; D – the dividing circle's diameter; d_n – the displacement of the rotor rotation axis in relation to the stator axis; δ – rotor displacement angle relative to the stator axis; b_n – the air gap. During operation, any defects that occur inside the bearing lead to certain radial movements between the stator and the rotor.

Disturbances that occur during the operation of the machine's electrical or mechanical parts and the mechanisms associated therewith lead to changes in the magnetic flux in the motor's air gap and affect the current being consumed. The use of the Fourier transform allows converting the signal presented in the temporal domain (current oscillogram) into the frequency domain [11,12].

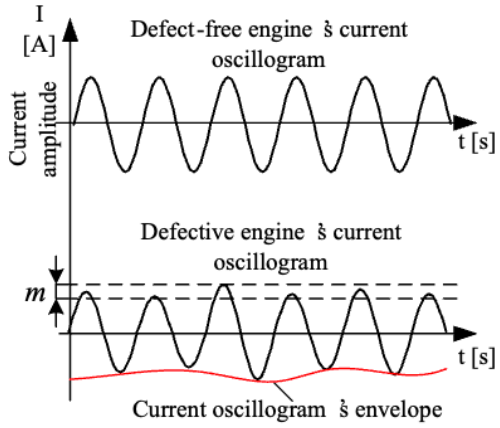

Fig. 2 – Current's periodic amplitude modulation in the temporal domain.

Figure 2 shows how the stator current's amplitude modulation occurs during oscillations caused by a mechanical defect. The current oscillogram's envelope is depicted as a dash-dotted line, the modulation depth *m* being shown as a dashed line. Thus, in the event of a defect in the machine, consumed current is additionally modulated by harmonic components, which leads to the appearance of additional harmonics and sub-harmonics in the frequency spectrum at different frequencies.

Each key element of the bearing has its own unique frequency at which energy is accumulated from cyclic loads and periodic shocks. These bearing frequency fluctuations may be determined in the following manner [10]:

- rotation bodies' rolling frequency along the inner ring:

$$f_i = \frac{n \cdot f_r}{2}\left(1 + \frac{d}{D}\cos(\beta)\right), \quad (1)$$

where *n* is the number of rolling elements;

f_r – the AE rotor's rotation frequency.

- the frequency of rolling bodies' rotation along the outer ring:

$$f_0 = \frac{n \cdot f_r}{2}\left(1 - \frac{d}{D}\cos(\beta)\right), \quad (2)$$

- the frequency of rolling elements' rotation:

$$f_0 = \frac{D \cdot f_r}{2d}\left(1 - \left(\frac{d}{D}\cos(\beta)\right)^2\right), \quad (3)$$

When the machine is running, only a few of the bearing's rolling elements obtain a direct static load, while the rest of the rolling elements roll between the cages. Loads alternately reach their maximum and minimum at the rolling elements' upper and lower points. These internal oscillations caused by defects in the machine's bearings lead to the appearance of certain harmonic components in the spectrum of the asynchronous engine's stator currents, which can be described by the following ratio [10,12]:

$$f_{ing} = (f_r + k \cdot f_d), \quad (4)$$

where f_d is one of the characteristic frequencies f_i, f_o, f_b of respective bearing oscillations (1)-(3), Hz; $k = \pm 1, 2, 3\ldots$ (the integers).

As a rule, induction motors with different heights of the rotation axis and different powers are operated in real facilities, and accordingly, bearings of different sizes are used. Therefore, to apply the above ratios (1)-(3), one should constantly recalculate the bearing frequencies, considering the design features of each size.

It is important to mention that bearing wear leads to the air gap eccentricity in the induction motor. This generates additional magnetic fields in the air gap, which, in turn, lead to the appearance of additional currents in the motor windings [11]. In such circumstances, it is important to consider the eccentricity's influence on the induction motor's operating mode.

In the three-phase stator winding, the magnetomotive force (MMF) of each individual phase presents the sum of harmonic components being stationary in space and pulsating in time [8]:

$$F_\Phi = \sum_{\nu=1,3,5} F_{\Phi\gamma m}\sin(\omega)\cos(\gamma\alpha), \quad (5)$$

where γ – the harmonic's number; ω – the harmonic's cyclic frequency, and $F_{\Phi\gamma m}$ – the amplitude of the magnetizing force of the spatial harmonics of respective order:

$$F_{\Phi\gamma m} = 0{,}9\frac{wK_{rot\gamma}}{\gamma p} I_\Phi, \quad (6)$$

where *w* – the number of turns in the phase winding; $K_{rot\gamma}$ –

the winding coefficient of the γ-th harmonic; I_Φ – the phase current.

The machine's resulting MMF for each separate harmonic component represents the sum of the respective harmonic components of the three phases. Under the conditions of stator and rotor windings' symmetry, and constant nature of the load at any time moment, the MMF generated by the currents of the third harmonica and a part of its "zero sequence" multiples (3, 9, 15,...) in three phase windings displaced relative to each other at the angle of 120°, coincide in phase, their sum equaling to zero [8]. In contrast to the said harmonics, the sum of MMFs of all other higher harmonics is not zero. The resulting MMF of such harmonic components is determined by expression [13]:

$$F_\gamma = F_{\Phi\gamma m}\sin(\omega t \pm \gamma\alpha). \quad (7)$$

In accordance with (7), the resulting MMF is characterized by an infinite number of higher harmonics *v*, each of which varies in space (sin(γα)) and time (sin(ωt)) according to the harmonic law. At the same time, the magnetic rotor's fields generated by intermediate paired symmetrical components of the MMF do not induce EMF in the stator winding [8,14].

According to the method of air gap's specific magnetic conductivity, the magnetic field in the air gap is determined by expression [8,11]:

$$B_\delta(\varphi, t) = F(\varphi, t)Y_b(\varphi, t), \quad (8)$$

where $F(\varphi,t)$ is the MMF in the air gap (generally equal to the sum of the MMF of the stator winding and the rotor winding); φ is the angular coordinate from the stator's inner circle; Y_b – the air gap's specific magnetic conductivity, considering the stator and rotor teeth (with a uniform air gap) is expressed by ratio [11]:

$$Y_b(\varphi, t) = \\ = \frac{\mu_0}{\delta_0}\left(\begin{array}{c} Y_0 + \sum_{k=1}^{\infty} Y_{zsk}\cos(kZ_s\varphi) + \\ + \sum_{k=1}^{\infty} Y_{zrk}\cos\left(kZ_s\left(\varphi - \frac{\omega_1 t(1-s)}{p}\right)\right) + \\ + \frac{1}{2}\sum_{k=1}^{\infty}\sum_{n=1}^{\infty} Y_{zsrk,n}\cos\left(\begin{array}{c}(kZ_r \pm nZ_s)\varphi - \\ -kZ_s\frac{\omega_1 t(1-s)}{p}\end{array}\right) \end{array}\right) \quad (9)$$

where μ_0 – the vacuum magnetic permeability; δ_0 – the nominal air gap between the stator and the rotor; Y_0 – the constant component of air gap conductivity; Y_{zs}, Y_{zr} – relative amplitudes of the *k*-th toothed harmonics of the stator and rotor air gap conductivity; Y_{zsr} – relative amplitudes of interference toothed conductivity harmonics caused by mutual movement of stator and rotor grooves; Z_s, Z_r – the number of the stator and rotor grooves; ω_1 – the supply voltage's cyclic frequency, and *s* – rotor slipping.

Air gap magnetic conductivity (9) contains the main elements of harmonics of Z_s and Z_r orders, which correspond to the stator and rotor slots, as well as mutual influence harmonics of $Z_r \pm Z_s$ orders.

In the presence of air gap eccentricity, conductivity harmonics additionally appear, which are determined by decomposition of the uneven gap's conductivity into the Fourier series [14, 15]:

$$Y_{b\varepsilon}(\varphi, t) = \frac{\mu_0}{\delta_0}\sum_{k=1}^{\infty}\lambda_k\cos(k\varphi), \quad (10)$$

where $Y_{k\,is}$ the amplitude of the k-th harmonic *of* the air gap conductivity.

Equation (10) is an additional term in formula (9), and besides, an uneven air gap also affects the values of the amplitude of conduction of the air gap's toothed harmonics λ_{zs}, λ_{zr} and λ_{zsr}.

In view of the aforesaid, we can conclude that the resulting mechanical malfunction leads to an increase in the number of spatial harmonics in the machine's gap. The most pronounced oscillatory forces are:

- the rotor's toothed harmonics conditioned by the presence of grooves in the rotor core:

$$f_{gr} = \frac{k\cdot Z_r}{p}f_r \pm \frac{f_r}{p}, \quad (11)$$

where Z_r is the number of rotor grooves (number of rods).

The stator's toothed harmonics are conditioned by the presence of grooves in the stator core:

$$f_{gs} = f_1\left(\frac{k\cdot Z_s}{p} \pm 1\right), \quad (12)$$

where k = 1, 2, 3 ... (the integers); Z_s – the number of stator slots, and p – the number of pole pairs.

Assuming that, as part of the bearing wear, the rotor's toothed harmonica directly interacts with the changes in magnetic conductivity in an uneven air gap due to the eccentricity, logical reasoning may lead to the conclusion that during defect development, this will primarily lead to a significant increase in its amplitude. Hence, in view of the foregoing, one can state that the bearings' wear contributes to the increase in the rotor's eccentricity degree, which in its turn leads to a periodic change in the air gap's magnetic conductivity and to the change in the harmonic composition of magnetic induction therein. On the grounds of the aforesaid, one can assume that bearings' wear contributes to the emergence of additional currents at frequencies kf_r, f_rk/p and $f_r(kZ_r/p \pm k/p)$.

5. EXPERIMENTAL RESEARCH OF AN INDUCTION MOTOR WHEN WORKING WITH EXISTING BEARING DEFECTS

A series of experimental trials was conducted using IM when working with defective and defect-free rolling bearings. During the experimental trial, the radial gap's following parameters were adopted for bearing 6205 [10]: nominal – 0.003-0.018 mm and maximum permissible – 0.08 mm.

To carry out the experimental trial, the experimental laboratory stand was developed, which is shown in Fig. 3.

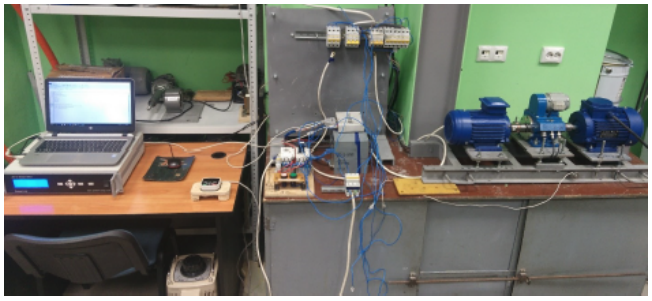

Fig. 3 – Experimental laboratory stand meant for experimental trials.

IM tests (AIR80A2) were conducted in two stages:
- defect-free bearings (radial clearance 0.035 mm);
- defective bearing (radial clearance 0.14 mm).

During the experimental trials, the bearings were

sequentially installed in the motor's front part, on its drive side. The trials were conducted under various mechanical loads, from idle to nominal, generated by a direct current generator. Amplitude-modulated frequencies were chosen in such a way as to correspond to the values of the maximum distortion during the development of a bearing assembly defect.

$$f_r k, \frac{f_r k}{p}, f_r\left(\frac{k \cdot z_r}{p} \pm \frac{k}{p}\right), \tag{13}$$

for AIR80A2 shown in Table 1.

Table 1

Amplitude-modulated frequencies corresponding to the maximum distortion during the development of a bearing unit defect in the asynchronous engine AIR80A2.

Load power [kW]	Rotor rotation frequency [Hz]	Frequencies of amplitude-modulated oscillations [Hz] (k = 1÷3, p = 1, Z_r = 16)								
		kf_r and kf_r/p			$f_r(k\ Z_r/p+ k/p)$			$f_r(k\ Z_r/p-k/p)$		
		k=1	k=2	k=3	k=1	k=2	k=3	k=1	k=2	k=3
0	49.83	49.83	99.66	149.49	847.11	1694.2	2541.3	747.45	1494.9	2242.4
0.5	49.11	49.11	99.22	147.33	834.87	1669.7	2504.6	736.65	1473.3	2209.9
1.0	48.25	48.25	96.5	144.75	820.25	1640.5	2460.7	723.75	1447.5	2171.3
1.5	47.5	47.5	95	142.2	807.5	1615	2422.5	712.5	1425	2137.5

Experimental amplitudes of harmonic components corresponding to the frequencies of the maximum distortion during defect development in the motor bearing unit obtained during investigation of spectral composition of the stator circuit's phase "1" current are shown in Tables 2, 3.

Table 2

Results of the experimental trial involving a defect-free bearing.

Load power [kW]	Stator current amplitude [A]	Frequencies of amplitude-modulated oscillations [Hz] (k = 1÷3, p = 1, Z_r = 16)								
		kf_r and kf_r/p			$f_r(k\ Z_r/p+ k/p)$			$f_r(k\ Z_r/p-k/p)$		
		k=1	k=2	k=3	k=1	k=2	k=3	k=1	k=2	k=3
0	0.1	0.0	0.0	0.0	0.0	0.0	0.0	0.001	0.0	0.0
0.5	1.64	0.004	0.001	0.001	0.002	0.001	0.001	0.007	0.002	0.001
1.0	3.26	0.005	0.001	0.001	0.001	0.001	0.0001	0.007	0.002	0.001
1.5	4.89	0.004	0.001	0.001	0.002	0.001	0.0001	0.009	0.002	0.001

Table 3

Results of the experimental trial involving a defective bearing.

Load power [kW]	Stator current amplitude [A]	Frequencies of amplitude-modulated oscillations [Hz] (k = 1÷3, p = 1, Z_r = 16)								
		kf_r and kf_r/p			$f_r(k\ Z_r/p+ k/p)$			$f_r(k\ Z_r/p-k/p)$		
		k=1	k=2	k=3	k=1	k=2	k=3	k=1	k=2	k=3
0	0.15	0.005	0.001	0.0	0.001	0.0	0.0	0.004	0.001	0.0
0.5	1.67	0.019	0.007	0.001	0.004	0.001	0.001	0.023	0.004	0.001
1.0	3.29	0.021	0.007	0.002	0.005	0.002	0.001	0.027	0.006	0.001
1.5	4.93	0.02	0.006	0.002	0.004	0.001	0.001	0.025	0.005	0.001

The results of experimental trials set forth in Tables 2, 3 fully confirm the foregoing theoretical conclusions regarding the distortion of the stator current shape in the presence of a bearing unit defect due to the increase in the amplitude of the frequencies calculated in accordance with (13).

6. **CONCLUSIONS**

The paper theoretically justified the impact characteristics of defects in induction motor bearings on its stator current waveform and demonstrated the potential use of the amplitudes of identified spectral components of the stator current as diagnostic indicators of bearing defects. It was shown that bearing wear leads to rotor slots harmonics due to eccentricity directly interacting with changes in magnetic conductivity in an uneven air gap, resulting in a significant increase in the amplitudes of harmonic components associated with the rotor rotational frequency.

Theoretical analysis established that bearing wear contributes to the amplification of current amplitudes at frequencies such as kfr, kfr/p and fr(kZr/p±k/p).

To validate the theoretical conclusions, experimental studies were conducted using defective and non-defective bearings with the induction motor АИР80А2. For the experiment, the bearings were sequentially installed in the front part of the motor, followed by an investigation of the spectral composition of the motor's stator current. The results of this experiment fully confirmed the theoretical conclusions.

The presence of an established functional relationship between the amplitudes of the spectral components of the stator current and the degree of wear of the bearings allows for the use of the amplitudes of the respective harmonic components as indirect diagnostic indicators of the technical condition of an induction motor. However, considering their ambiguity, the use of such indicators may have practical significance only when combined with other diagnostic indicators (such as vibration, magnetic, etc.) as part of a comprehensive assessment of the technical condition of the induction motor.

CREDIT AUTHORSHIP CONTRIBUTION STATEMENT

VALERII HRANIAK: conceptualization, formal analysis, investigation (experiment), methodology, writing (draft, review, and editing).

VASYL PONOMARENKO: formal analysis, visualization, investigation (methodology of experiment), software (DAQ).

Received on 16 September 2025

REFERENCES

1. H.W. Beaty, J.L. Kirtley, *Electric motor handbook*, McGraw-Hill, New York, pp. 1–400 (1998).
2. V. Hraniak, *Using discrete wavelet analysis of vibration signal for detection of electrical machines' defects*, Rev. Roum. Sci. Techn. – Électrotechn. et Énerg., **68**, *4*, pp. 357–362 (2023).
3. V.D. Voitiuk, *Theoretical substantiation of objects and means of diagnosis during their certification: monograph*, Center for Educational Literature, Kyiv, pp. 1–264 (2022).
4. I.V. Khomenko, O.A. Plakhtii, V.P. Nerubatskyi, I.V. Stasiuk, *Electricity of Ukraine. Structure, management, innovations: monograph*, Planeta-Print, Kharkiv, pp. 1–132 (2020), http://lib.kart.edu.ua/bitstream/123456789/4892/1/Монографія.pdf
5. M.-D. Drid, S. Hamdani, A. Nait-Seghir, L. Chrifi-Alaoui et al., *Fault-tolerant, capable and scalable two-time-scale boost converter meant for residential areas*, Rev. Roum. Sci. Techn. – Électrotechn. et Énerg., **70**, *3*, pp. 373–378 (2025).
6. ****Vettus*, *Problems in the operation of an asynchronous electric motor*, Kyiv, pp. 1–10 (2025), https://www.ventus.kiev.ua/неполадки-в-работе-асинхронного-электродвигателя/.
7. I. Honcharuk, I. Kupchuk, V. Yaropud, R. Kravets et al., *Mathematical modeling and creation of algorithms for analyzing the ranges of the amplitude-frequency response of a vibrating rotary crusher in the software Mathcad*, Przeglad Elektrotechniczny, **98**, *9*, pp. 14–20 (2022).
8. F. Allythi, *Three-phase asynchronous motors*, Noor Publishing, London, pp. 1–200 (2020).
9. A.G. Yetgin, M.M. Tezcan, *Effect of the lambda parameter on three-phase induction motor design by analytical and magnetic methods*, Rev. Roum. Sci. Techn. – Électrotechn. et Énerg., **70**, *4*, pp. 435–440 (2025).
10. L. Hasbargen, J. Brindlein, K. Weigand, P. Eschmann, *Ball and roller bearings: Theory, design and application*, John Wiley & Sons, New Jersey, pp. 1–644 (1999).
11. A.I. Kupin, D.I. Kuznietsov, *Information technology for group diagnosis of asynchronous electric motors based on spectral characteristics and intelligent classification*, Publisher of FOP Chernyavskyi D.O., Kryvyi Rih, pp. 1–200 (2016).
12. V.V. Kukharchuk, S.Sh. Katsyv, V.F. Hraniak, V.G. Madyarov et al., *Analysis of dependency current harmonics on load and filter parameters for asymmetrical network models*, Przeglad Elektrotechniczny, **96**, *9*, pp. 103–107 (2020).
13. G.A. Sziki, A. Szanto, J. Kiss, G. Juhasz et al., *Measurement system for the experimental study and testing of electric motors at the faculty of engineering, University of Debrecen*, Applied Sciences, **12**, *19*, pp. 1–18 (2022).
14. M.E. El-Hawary, *Principles of electric machines with power electronic applications*, John Wiley & Sons, Newark, pp. 1–862 (2002).
15. K.M.S. Benzaoui, E. Benyoussef, A.Z. Kouache, *Three-level direct torque control based on common mode voltage reduction strategy fed two parallel connected five-phase induction machine*, Rev. Roum. Sci. Techn. – Électrotechn. et Énerg., **69**, *2*, pp. 177–182 (2024).